

## **Influence of Temperature and Shear Rate on the Slip Length in the Hydrodynamic Lubrication for a Polyalphaolefin**

Tobias Corneli, M.Sc., Univ.-Professor Dr.-Ing. Peter F. Pelz , Dr.-Ing. Gerhard Ludwig, Institut für Fluidsystemtechnik (FST), Technische Universität Darmstadt

### **1. Introduction**

Generally sealing systems are designed by means of elasto-hydrodynamics. In this case, the no slip boundary condition is applied to the solid walls for solving the Reynolds equation. Nowadays engineers apply the no-slip boundary condition with the most matter of course. But in the 19<sup>th</sup> century the behaviour of fluids close to the solid wall was discussed by personalities as Stokes, Poisson, Maxwell or Navier. Navier [1] e.g. introduced a slippage factor in his derivation of the Navier-Stokes equations.

In the middle of the 19<sup>th</sup> century Stokes was commissioned by the Royal Society, to discuss the issue regarding the slipping behaviour of fluids close to solid walls. And he concluded in [2] & [3] that the effect of slippage on solid walls, if it exists, was up to his time too small to measure and could be neglected. Hence for sufficiently large flow geometries the effect of wall sliding was neglected. Even today measuring the slip velocity close to solid walls is a challenging task and no general approach has figured out. This conclusion yields up to now and is sometimes treated like a principle. But in the case of sealing systems where commonly gaps are in the order of some microns and below the effect of wall slippage has to be taken into account. Experimental investigations of sealing manufacturers show that the leakage behaviour of geometrically identical sealing systems depends on the material pairing and hence on the surface energy. As a cause for the discrepancy between calculations and experimental investigations a breakdown of the no slip boundary condition is suspected.

Reprinted with permission from [Corneli, T. ; Pelz, P. F. ; Ludwig, G. (2016): Influence of Temperature and Shear Rate on the Slip Length in the Hydrodynamic Lubrication for a Polyalphaolefin. In: 19th International Sealing Conference, 12.10. - 13.10. 2016, Stuttgart]. Copyright 2022 VDMA Fluidtechnik

Licence: CC BY 4.0 / Creative Commons Attribution 4.0 International

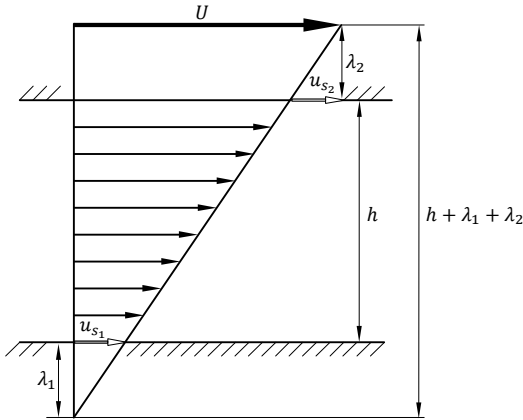


Figure 1: Linear boundary condition for a simple shear flow.

The breakdown of the no slip condition is related to the violated continuum hypothesis: In narrow sealing gaps on the scale of a few microns must be considered that the continuum hypothesis is no longer applicable. For the case of slippage close to the solid wall Hermann von Helmholtz introduced in 1860 [4] the linear boundary condition. Such a behaviour is illustrated for a simple shear flow in *Figure 1*. In this sketch the lower wall is at rest and the upper one is moved by the constant velocity  $U$ . Due to the slippage the fluid close to the stationary wall moves with the slip velocity  $u_{s1} > 0$  and the fluid velocity close to the moving wall is reduced by the slip velocity  $u_{s2}$ . The linear boundary condition is obtained if the fluid velocity profile in the gap is linearly extrapolated up to the case of no slip. This means at the stationary wall down to zero and at the moving wall up to wall velocity  $U$ . The normal distance between the wall and the extrapolated velocity profile represents the slip length  $\lambda_1$  and  $\lambda_2$ . From this sketch the geometrical interpretation of wall slip as an apparent gap opening can be figured out.

Slip velocity  $u_s$  and shear rate  $\dot{\gamma}$  are linked by the slip length  $\lambda$ :

$$u_s = \lambda \dot{\gamma} \quad (1)$$

Up to now slip length measurements were mainly performed for long-chain silicone molecules and water. Regarding the solid surfaces glass and silicon wafers were mainly used. The purpose of these up to now applied measurement methods is mostly limited to a few tribological systems - which are not directly related to common hydraulic systems. A review is given by the authors in [5].

## 2. Measurement Principle

In this section, the measurement approach for determining the slip length of a typical material combination of hydraulics, is presented in detail.

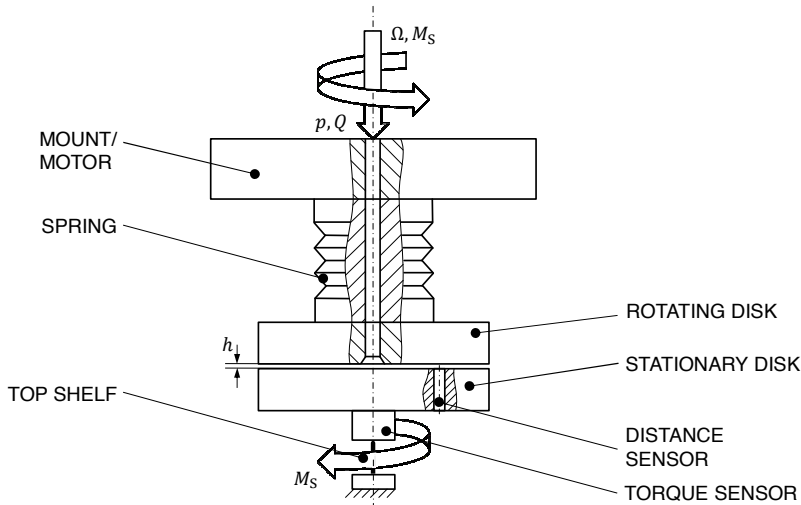


Figure 2: Measurement principle – Experimental setup.

Figure 2 shows a principle sketch of the measurement device. Key parts are the rotating and the stationary disk. The measuring apparatus evaluates the torque that is transferred from the rotating to the stationary disc through the liquid film depending on the gap height  $h$ . The gap height is adjusted by the inlet pressure  $p$  and the stiffness as well as the initial load of the spring. The measurement of the gap is realized by a capacitive distance sensor that is integrated into the stationary disk. The top shelf resembles the wobbling motion of the power train due to the bearing play of the used roller bearings. Figure 3 illustrates the experimental examination of the slip length. The measurement principal was developed by Pelz in 2007 and was already published in [6].

The transmitted torque is applied to the accompanying gap height. The torque at  $h=0$  can not be measured due to the fact that each technical surface has a finite roughness. Measurements at a sufficient number of measurement points allow the determination of the torque at gap height  $h=0$  by an extrapolation of the recorded measurement points.

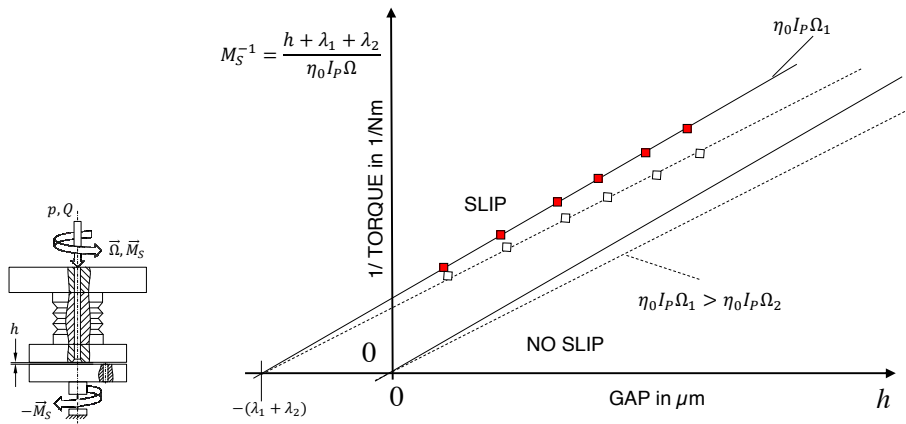


Figure 3: Measurement principle – Analysis of the slip length. [6]

From hydrodynamic lubrication theory it is known that the friction torque between two flat disks at distance  $h$  for no slip boundary condition is given by the equation

$$M = \frac{\eta \Omega I_p}{h}. \quad (2)$$

In the above equation  $\eta$  represents the dynamic viscosity,  $\Omega$  the rotational speed of the disk and  $I_p$  the geometrical moment of inertia. From equation (2) it can be figured out that the friction torque  $M$  is an inverse linear function of the gap height  $h$ . This relationship is illustrated in *Figure 3* with the markers for the case of slippage. The inverse friction torque remains finite for zero gap height. For the case of no slip, denoted by the lines without markers, the inverse friction torque tends to zero for zero gap height. With an increasing rotational speed of the rotating disk, the inclination of the linear function increases. The red and the white markers denote two different rotational speeds at constant dynamic viscosity and equal geometry. Above it was mentioned that the slip length can be interpreted as an enlargement of the confined gap.

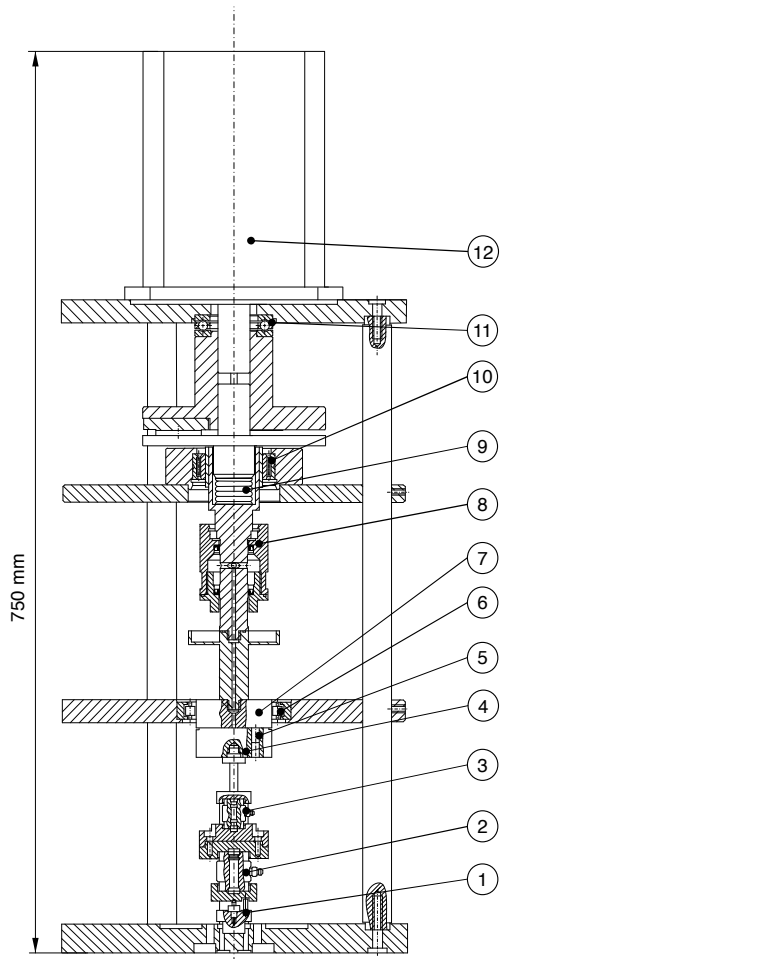
For the presented test rig, slip occurs at the rotating as well as at the stationary disk.  $\lambda_1$  represents the gap enlargement due to the surface at the stationary disk and  $\lambda_2$  the enlargement due to the surface at the rotating disk. And the sum of the slip length is evaluated by an extrapolation of the inverse frictional torque until the linear line crosses the abscissa. The negative axis section indicates the sum of the slip length of the fixed and rotating disk. Furthermore *Figure 3* contains the hypothesis that the slip length is independent of the shear rate  $\dot{\gamma}$ . This hypothesis has to be proofed by experimental investigations.

### 3. Test Rig

In this section the design implementation of the slip length tribometer is described in detail. For a better understanding the sketch from *Figure 2* is recapped. The slip length is obtained by the measurement of the two quantities gap height  $h$  and frictional torque  $M$ . The key parts of the test rig are the two gap confining disks and the top shelf.

In

*Figure 4* a sectional view of the test rig is presented. The main components that ensure the function of the tribometer are labeled with numbers and named in the table stated below the sectional view. The test rig can be roughly subdivided into two parts: the drivetrain (No. 1 to 4) and the powertrain (No. 5 to 12). The drivetrain contains the measurement devices: The torque sensor with a maximum measurement range of 1 Nm, the force sensor to adjust the spring preload and the capacitive distance sensor with a measurement range of 200  $\mu\text{m}$ . The mounting of the distance sensors will be discussed later on. The powertrain contains the supply. The fluid is fed into the system by a rotary feed through. This has the advantage that the measurement chain (drivetrain) remains torque-free. A synchronous servo drive with a maximum torque of 10 Nm is used to provide a constant rotational speed. The powertrain is beard by a conventional fixed-floating bearing. The remaining clearance of the roller bearings is adjusted by a gimbal mounting of the drive train. This is obtained by the top shelf.



- |   |                 |    |                                |
|---|-----------------|----|--------------------------------|
| 1 | TOP SHELF       | 7  | ROTATING DISK                  |
| 2 | FORCE SENOR     | 8  | ROTARY FEEDTHROUGH             |
| 3 | TORQUE SENSOR   | 9  | SPRING                         |
| 4 | STATIONARY DISK | 10 | NEEDLE BEARING                 |
| 5 | DISTANCE SENSOR | 11 | AXIAL DEEP GROOVE BALL BEARING |
| 6 | ROLLER BEARING  | 12 | MOTOR                          |

Figure 4: TU Darmstadt slip length tribometer.

Of paramount importance for the tribometer are the lubricating gap and the gap measurement. The gap confining disks are made by a nitrided steel. In a first step the disks were drilled with a definite material allowance. Subsequently they were hardened and dressed to size. These blanks are displaced by the manufacturing process lapping into the final state. The finished disks have a flatness of 30 nm.

The distance measurement system is directly inserted into the stationary gap confining disk and calibrated by the sensor manufacturer after the finishing of the disks.

#### 4. Results

In this section the obtained results are presented. In a first step the reproducibility of the measurement results was focused in the investigations. The temperature during the measurements was kept constant by  $\pm 0.1^\circ\text{C}$ . This is reached due to the fact that the whole test rig is operated in a commercial temperature chamber. The measurements were conducted at  $40^\circ\text{C}$  using a polyalphaolefin with a kinematic viscosity of  $\nu = 29 \text{ mm}^2/\text{s}$ .

*Figure 5* show the results of five slip length measurements at two rotational speeds. Two measurements were conducted at rotational speeds of 1 Hz and three at rotational speeds of 1.5 Hz. The left part of *Figure 5* shows the different measurement points across the varying gap height. Each marker represents one torque measurement. The minimum reached gap height was about  $1.3 \mu\text{m}$ .

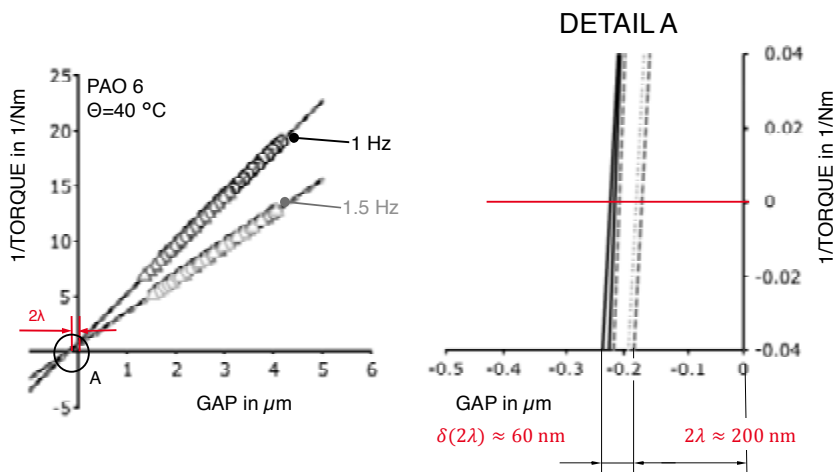


*Figure 5*: Slip length measurements.

On the left diagram there is nearly no difference in reproducibility for the different measurements recognizable. Hence a closer look at the intersection with the abscissa is

useful and illustrated in the right diagram of *Figure 5*. In this detail view one can figure out, that the difference in the sum of the slip length measurements varies by  $\pm 30$  nm. These results are satisfactory and a good basis for the beginning of systematic investigations.

## 5. Summary and Outlook

In this paper a method and a tribometer to evaluate the slip length with regard to an usage in hydraulic applications was presented. This quantity allows sealing manufacturers to understand the relation between surface energy and leakage behaviour of sealing systems. Up to now at the Chair of Fluid Systems the measurement principle was developed and applied for the tribological system steel-polyalphaolefin-steel at one constant temperature. For the future these investigations have to be extended and systematized. In a first step the temperature has to be varied from 10°C to 80°C. Based on these investigations two easy possibilities exist to influence the tribological system. First the synthetic oil can be changed into a mineral based hydraulic oil. And the surface energy of the gap confining disk can be reversible changed by a plasma treatment.

## 6. Acknowledgement

The authors thank the Research Association for Fluid Power of the German Engineering Federation VDMA for its financial support. Special gratitude is expressed to the participating companies and their representatives in the accompanying industrial committee for their advisory and technical support.



## 7. Literature

- [1] M. Navier, “Sur les lois du Movement des Fluides”, *Mémoires de l'Academie royal des Sciences de l'Institut de France*, 1822.
- [2] G. G. Stokes, “Report on Recent Researches in Hydrodynamics”, *Mathematical and Physical Papers*, Volume 1, 1846.
- [3] G. G. Stokes, “On the Theories of the Internal Friction of Motion, and the Equilibrium and Motion of elastic solids”, *Mathematical and Physical Papers*, Volume 1, 1845.
- [4] H. Helmholtz and G. Piortrowski. “Über Reibung tropfbarer Flüssigkeiten”, *Sitzungsberichte der Kaiserlichen Akademie der Wissenschaften mathematisch-naturwissenschaftlichen Classe*, 40, Abteilung 2, 1860.
- [5] T. Corneli, G. Ludwig and P. F. Pelz - “Slip length of the tribo system steel-polyalphaolefin-steel determined by a novel tribometer”, *10th International Fluid Power Conference, Dresden, Germany* pp. 479-491, 2016.
- [6] T. Corneli, G. Ludwig and P. F. Pelz - “Slip length in narrow sealing gaps – an experimental approach”, *18th International Sealing Conference, Stuttgart*, 2016.

## 8. Nomenclature

$h$	gap height
$I_p$	geometrical moment of inertia
$M$	frictional torque
$p$	pressure
$U$	wall velocity
$u_s$	slip velocity
$\dot{\gamma}$	shear rate
$\eta$	dynamic viscosity
$\lambda$	slip length
$\nu$	kinematic viscosity
$\Omega$	rotational speed